Biochemical Characterization and Identification of the Catalytic Residues of a Family 43 β-D-Xylosidase from *Geobacillus stearothermophilus* T-6†

Dalia Shallom,‡ Maya Leon,‡ Tsafrir Bravman,‡ Alon Ben-David,‡ Galia Zaide,‡ Valery Belakhov,§ Gil Shoham,||,¶ Dietmar Schomburg,⊥ Timor Baasov,§,# and Yuval Shoham*,‡,#

Department of Biotechnology and Food Engineering, Technion—Israel Institute of Technology, Haifa 32000, Israel, Department of Chemistry, Technion—Israel Institute of Technology, Haifa 32000, Israel, Institute of Catalysis Science and Technology, Technion—Israel Institute of Technology, Haifa 32000, Israel, Department of Inorganic Chemistry and The Laboratory for Structural Chemistry and Biology, The Hebrew University of Jerusalem, Jerusalem 91904, Israel, and Institute for Biochemistry, University of Cologne, Cologne 50674, Germany

Received September 9, 2004; Revised Manuscript Received October 20, 2004

ABSTRACT: β-D-Xylosidases are hemilcellulases that hydrolyze short xylooligosaccharides into xylose units. Here, we describe the characterization and kinetic analysis of a family 43 β-xylosidase from *Geobacillus stearothermophilus* T-6 (XynB3). Enzymes in this family use an inverting single-displacement mechanism with two conserved carboxylic acids, a general acid, and a general base. XynB3 was most active at 65 °C and pH 6.5, with clear preference to xylose-based substrates. Products analysis indicated that XynB3 is an exoglycosidase that cleaves single xylose units from the nonreducing end of xylooligomers. On the basis of sequence homology, amino acids Asp15 and Glu187 were suggested to act as the general-base and general-acid catalytic residues, respectively. Kinetic analysis with substrates bearing different leaving groups showed that, for the wild-type enzyme, the k_{cat} and k_{cat}/K_m values were only marginally affected by the leaving-group reactivity, whereas for the E187G mutant, both values exhibited significantly greater dependency on the pK_a of the leaving group. The pH-dependence activity profile of the putative general-acid mutant (E187G) revealed that the protonated catalytic residue was removed. Addition of the exogenous nucleophile azide did not affect the activities of the wild type or the E187G mutant but rescued the activity of the D15G mutant. On the basis of thin-layer chromatography and ^{1}H NMR analyses, xylose and not xylose azide was the only product of the accelerated reaction, suggesting that the azide ion does not attack the anomeric carbon directly but presumably activates a water molecule. Together, these results confirm the suggested catalytic role of Glu187 and Asp15 in XynB3 and provide the first unequivocal evidence regarding the exact roles of the catalytic residues in an inverting GH43 glycosidase.

β-D-Xylosidases (EC 3.2.1.37) hydrolyze β-1,4 glycosidic bonds between two xylose (X_1)[1] units in short xylooligosaccharides. These enzymes are part of an array of hemicellulases responsible for the complete degradation of xylan, the most abundant hemicellulose in the plant cell wall. Hemicellulases are utilized in many biotechnological applications, and their structure−function relationships are a subject of intense research in recent years (*1*−*3*).

The spontaneous hydrolysis of O-glycosidic bonds at room temperature is extremely slow, and their half-life is estimated to be over 5 millions years (*4*). The enzymes that mediate the hydrolysis of glycosidic bonds, glycosidases, may accelerate this reaction by more than 10^{17}-fold, making them among the most efficient catalysts known. The enzymatic hydrolysis of the glycosidic bonds proceeds through two major mechanisms, resulting in either an overall retention or an inversion of the anomeric configuration of the sugar. In both mechanisms, the hydrolysis usually requires two carboxylic acids and proceeds through oxocarbenium-ion-like transition states. Retaining glycosidases use a double-

† This study was supported by grants from G.I.F., the German−Israeli Foundation for Scientific Research and Development (to Y.S., T.B., D.S., and G.S.), from the French−Israeli Association for Scientific and Technological Research (AFIRST) (to Y.S.), and from the Israel Science Foundation (to G.S. and Y.S.). Additional support was provided by the Otto Meyerhof Center for Biotechnology, Technion, established by the Minerva Foundation (Munich, Germany). V.B. acknowledges the financial support by the Center of Absorption in Science, the Ministry of Immigration Absorption, and the Ministry of Science and Arts, Israel (Kamea program).

* To whom correspondence should be addressed: Department of Biotechnology and Food Engineering, Technion, Haifa 32000, Israel. Telephone: 972-4-8293072. Fax: 972-4-8293399. E-mail: yshoham@tx.technion.ac.il.

‡ Department of Biotechnology and Food Engineering, Technion—Israel Institute of Technology.

§ Department of Chemistry, Technion—Israel Institute of Technology.

|| The Laboratory for Structural Chemistry and Biology, The Hebrew University of Jerusalem.

⊥ University of Cologne.

Institute of Catalysis Science and Technology, Technion—Israel Institute of Technology.

¶ Department of Inorganic Chemistry, The Hebrew University of Jerusalem.

[1] Abbreviations: X_1, xylose; GH, glycoside hydrolase; XynB3, family 43 β-D-xylosidase from *Geobacillus stearothermophilus* T-6; BSA, bovine serum albumin; pNPX, 4-nitrophenyl β-D-xylopyranoside; $pNPX_2$, 4-nitrophenyl β-D-xylobioside; DMSO, dimethyl sulfoxide; TLC, thin-layer chromatography; NMR, nuclear magnetic resonance; Arb43A, α-L-arabinanase from *Cellvibrio japonicus*; pNP, 4-nitrophenol; X_2, xylobiose; X_3, xylotriose; X_4, xylotetraose; X_5, xylopentaose; X_6, xylohexaose.

10.1021/bi048059w CCC: $30.25
Published on Web 12/03/2004

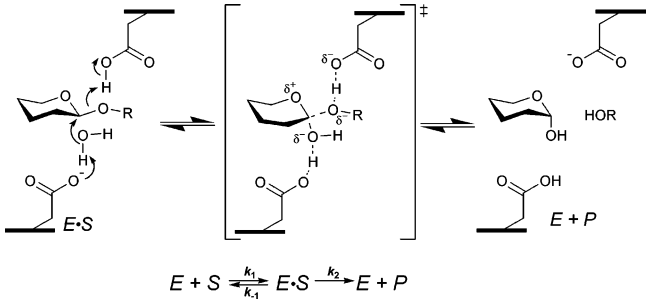

FIGURE 1: Proposed mechanistic pathway of inverting glycosidases.

displacement mechanism, where one catalytic residue functions as a nucleophile and the other as a general acid−base. Inverting glycosidases operate through a single displacement mechanism, in which usually one carboxylic acid acts as a general acid and one as a general base (*5*, *6*) (Figure 1). Currently, more than 12 600 glycosidase sequences are known, and the sequence-based classification of their catalytic domains into glycoside hydrolase (GH) families and clans is available on the continuously updated Carbohydrate-Active Enzymes (CAZy) server (http://afmb.cnrs-mrs.fr/CAZY). β-Xylosidases are found in the retaining GH families 3, 39, 52, and 54 and in the inverting GH family 43.

GH43 family, which is assigned together with family GH62 to clan GH-F, includes enzymes with different substrate specificities such as β-xylosidases, α-L-arabinofuranosidases, arabinanases, and xylanases. The crystal structure of the α-L-arabinanase Arb43A from *Cellvibrio japonicus* is currently the only 3D structure of a GH43 glycosidase (*7*). This structure revealed a five-bladed β-propeller fold, and it was the first demonstration of such enzyme topology. More recently, this kind of topology was observed also for the GH32 invertase from *Thermotoga maritime* and the GH68 levansucrase from *Bacillus subtilis* (*8*, *9*). Both of these enzymes are retaining glycosidases that belong to clan GH-J. The similarity between glycosidases of GH-J and GH-F clans was noted before the crystal structures were available, on the basis of protein sequence comparisons that showed several conserved blocks in these enzymes (*10*−*12*). One of the most characterized β-xylosidases is from *Bacillus pumilus* PRL B12. This enzyme was subjected to detailed mechanistic studies, including binding experiments of various substrates, α-deuterium kinetic isotopic effect measurements, inhibition studies, and hydrolysis of different aryl-β-D-xylopyranosides (*13*−*17*). Unfortunately, the protein sequence of this enzyme and therefore its GH classification was never determined. However, because this enzyme is an inverting glycosidase, it is likely that it belongs to family GH43 (*18*).

Geobacillus stearothermophilus T-6 is a thermophilic bacteria that was originally isolated based on its ability to produce alkaline-tolerant, thermostable xylanases that could be used in biobleaching of wood pulp (*19*) and since then was shown to have an extensive hemicellulolytic system (*3*, *20*). Two β-xylosidases from *G. stearothermophilus* T-6, XynB1 from GH39 and XynB2 from GH52, were previously isolated and fully characterized (*21*−*24*). Here, we report the isolation and characterization of a third β-xylosidase from this strain, XynB3, which belongs to the inverting GH43. The catalytic residues of the enzyme were identified by a combination of several independent techniques, including detailed kinetic analysis with substrates bearing different leaving groups, pH-dependence activity profiles, and azide rescue of activity. These techniques are often used with retaining glycosidases, but their exploitation for the identification of the catalytic residues of inverting glycosidases was only seldom described. The results provide the first unequivocal evidence regarding the exact role of each of the catalytic residues in an inverting GH43 glycosidase.

MATERIALS AND METHODS

Cloning, Mutagenesis, Protein Expression, and Purification of XynB3. The *xynB3* gene (GenBank accession number AY690618) was amplified from genomic DNA of *G. stearothermophilus* T-6 by a PCR reaction (N-terminal primer: 5′-AAAGGGGGACGAGTACCC**ATG**GCCAAAATCAAAAATCC-3′; C-terminal primer: 5′-GCTTCGGTTTTATTGGATCCCTTTCACATTTGTTTG-3′) and cloned into the T7 polymerase expression vector pET9d (Novagen).

Site-directed mutagenesis was performed using the QuikChange site-directed mutagenesis kit (Stratagene), using the wild-type pET9d-*xynB3* as the template. The mutagenic primers were as follows (the mutated nucleotides are shown in bold): E187G, 5′-CTTAAGAATTACAG**GT**GGGCC-**C**CATTTGTATAAAATC-3′ and 5′-GATTTTATACAAATG**G**GGCCC**AC**CTGTAATTCTTAAG-3′; D128G, 5′-CAGCTCTGGATTTG**GG**CC**C**TCTCTTTTTCATGATG-3′ and 5′-CATCATGAAAAAGAGA**G**GG**CC**CAAATCCAGAGCTG-3′; D15G, 5′-GCTTCCATCCCG**GG**CC**C**TCCATTTGCCG-3′ and 5′-CGGCAAATGGA**G**GG**CC**CGGGATGGAAGC-3′. The mutated genes were sequenced to confirm that only the desired mutations were inserted.

Expression of the *xynB3* gene or its mutants was carried out by growing overnight cultures of *Escherichia coli* BL21-(DE3) carrying pET9d-*xynB3* in Terrific Broth medium (*25*) (500 mL in 2 L shake flasks, shaken at 220 rpm and 37 °C), supplemented with kanamycin (25 μg/mL), without induction. After growth, cells from 1 L of overnight culture (OD_{600} of 14−18) were harvested (14000*g* for 10 min), resuspended in about 55 mL of 50 mM Tris-HCl at pH 7.0, 100 mM NaCl, and 0.02% NaN_3, and disrupted by two passages through a French-Press (Spectronic Instruments, Inc.) at room temperature. The cell extract was centrifuged (14000*g* for 15 min), and the soluble fraction was heat-treated (at 60 °C for 30 min) and centrifuged again at room temperature. The soluble fraction (about 50 mL) contained the recombinant XynB3 as the main product at a concentration of about 20 mg/mL. Final purification of the enzyme was performed by gel filtration using a Superdex 200 26/60 column, AKTA explorer (Pharmacia), running at 2.5 mL/min with 50 mM Tris-HCl buffer at pH 7.0, 100 mM NaCl, and 0.02% NaN_3. The enzymes appeared as distinct protein peaks, which were then collected and used for biochemical characterization. Protein concentrations were determined by the Bradford method, with bovine serum albumin (BSA) as a standard (*26*).

Substrates. 4-Nitrophenyl β-D-xylopyranoside (pNPX), 4-methylumbelliferyl β-D-xylopyranoside, and all of the 4-nitrophenyl glycosides were obtained from Sigma Chemical Co. 4-Bromophenyl β-D-xylopyranoside and 3,4-dimethylphenyl β-D-xylopyranoside were obtained from Charlock Enterprises Ltd. (London, U.K.). Xylooligosaccharides

were purchased from MegaZyme Ltd. (Bray, Republic of Ireland). 2,5-Dinitrophenyl β-D-xylopyranoside, 3,4-dinitrophenyl β-D-xylopyranoside, and 3-nitrophenyl β-D-xylopyranoside were synthesized as described by Ziser et al. (*27*). 2-Naphthyl β-D-xylopyranoside was synthesized as described in Bravman et al. (*23*). 4-Nitrophenyl β-D-xylobioside ($pNPX_2$) was synthesized as described previously (*28*).

Kinetic Studies. Steady-state kinetic studies were performed by following the spectroscopic absorbance changes in the UV−visible range, using an Ultrospec 2100 *pro* spectrophotometer (Pharmacia) equipped with a temperature-stabilized water-circulating bath. All substrates were initially dissolved in dimethyl sulfoxide (DMSO), and the reaction contained DMSO in a final concentration of 10% (v/v). Initial hydrolysis rates were determined by incubating 500 μL of different substrate concentrations in 100 mM phosphate buffer at pH 7.0 and 40 °C within a water-heated cell in the spectrophotometer, until thermal equilibration was achieved. Reactions were initiated by the addition of 200 μL of appropriately diluted enzyme containing 1 mg/mL BSA. The release of the phenol-derived product was monitored at the appropriate wavelength. For highly reactive substrates, blank mixtures containing all of the reactants except the enzyme were used to correct for spontaneous hydrolysis of the substrates. The extinction coefficients used and wavelength monitored for each substrate at pH 7.0 were as follows: 2,5-dinitrophenyl, 420 nm, $\Delta\epsilon = 3.68\ mM^{-1}\ cm^{-1}$; 3,4-dinitrophenyl, 400 nm, $\Delta\epsilon = 11.15\ mM^{-1}\ cm^{-1}$; 4-nitrophenyl, 420 nm, $\Delta\epsilon = 7.61\ mM^{-1}\ cm^{-1}$; 4-methylumbelliferyl, 355 nm, $\Delta\epsilon = 2.87\ mM^{-1}\ cm^{-1}$; 3-nitrophenyl, 380 nm, $\Delta\epsilon = 0.455\ mM^{-1}\ cm^{-1}$; 4-bromophenyl, 289 nm, $\Delta\epsilon = 0.626\ mM^{-1}\ cm^{-1}$; 2-naphthyl, 330 nm, $\Delta\epsilon = 0.871\ mM^{-1}\ cm^{-1}$; 3,4-dimethylphenyl, 285 nm, $\Delta\epsilon = 0.90\ mM^{-1}\ cm^{-1}$. Values of K_m and k_{cat} were determined by nonlinear regression analysis using GraFit 5.0 (*29*). In cases where the K_m values were too high to be estimated, k_{cat}/K_m values were calculated from the reaction rates at low substrate concentrations ($[S] \ll K_m$).

The effect of various metal ions on the activity of XynB3 was investigated by adding 0.1 or 1 mM of various salts or EDTA to the standard activity assay. Activity rescue experiments were performed by adding different concentrations of sodium azide to the standard activity assay.

pH-dependence studies were carried out at 40 °C with pNPX as a substrate. Mixtures containing 600 μL of different concentrations of substrate solutions in the appropriate buffer were prewarmed until the reaction was initiated by the addition of 200 μL of appropriately diluted enzyme containing 1 mg/mL BSA. The buffers used were at final concentrations of 100−200 mM and were citric acid−Na_2HPO_4 (pH 2.6−7.2), phosphate buffer (pH 5.8−8.0), Tris-HCl buffer (pH 7.5−9.0), and sodium carbonate−sodium bicarbonate (pH 9.2−10.2) (*30*). The pH range employed in this study included only pH values for which the enzyme was stable for at least 5 min. Reactions were monitored continuously, and upon completion, the actual pH was measured to verify that the pH had not changed. Extinction coefficients of 4-nitrophenol were determined at each pH, and values of K_m, k_{cat}, and k_{cat}/K_m were determined as described above. The pH-dependence plots and the pK_a values assigned to the ionizable groups were determined using GraFit 5.0.

The effect of temperature on the reaction rate was determined by performing the standard reaction with pNPX as a substrate in 100 mM sodium citrate buffer (pH 5.0) for 20 min at different temperatures ranging from 30 to 75 °C. The thermostability of XynB3 was determined after incubating the purified enzyme for 10, 20, and 30 min at different temperatures in 100 mM sodium citrate buffer (pH 5.0), in the presence of 1 mg/mL BSA. The residual activity was measured with pNPX at 40 °C and pH 5.0. The extinction coefficients of 4-nitrophenol at pH 5.0 were determined at each temperature.

Thin-Layer Chromatography (TLC). The hydrolysis of xylohexaose and $pNPX_2$ by the wild-type XynB3 and the hydrolysis of pNPX by the D15G mutant in the presence of sodium azide were monitored by TLC analysis. The xylohexaose hydrolysis reaction included 8.3 mM xylohexaose and 0.3 mg/mL XynB3. The $pNPX_2$ hydrolysis reaction included 1.5 mM $pNPX_2$ and 0.02 mg/mL XynB3. The pNPX hydrolysis reaction by D15G included 40 mM pNPX, 0.375 M sodium azide, and 2 mg/mL D15G XynB3. All three reactions were performed at 40 °C and 100 mM phosphate buffer (pH 7.0). At different time points, samples were taken and the reactions were stopped by either boiling the sample or by adding Hg^{2+} to a final concentration of 1 mM (which completely inhibits the enzyme). Chromatography was carried out on silica gel 60 plates (Merck), using EtOAc/MeOH/H_2O (6:3:1) as a developing solvent. Spots were visualized by charring with yellow solution containing (NH_4)-$Mo_7O_{24}\cdot 4H_2O$ (120 g) and $(NH_4)_2Ce(NO_3)_6$ (5 g) in 10% H_2SO_4 (800 mL).

^{1}H Nuclear Magnetic Resonance (NMR). The hydrolysis of pNPX by D15G in the presence of sodium azide was monitored by ^{1}H NMR on a Bruker Avance 500 MHz spectrometer. The mutant enzyme D15G was dialyzed against a 5 mM triethanolamine hydrochloride buffer at pH 6.0 and 30 mM NaCl, lyophilized, and resuspended in D_2O. pNPX and sodium azide were dissolved in deuterated buffer (5 mM triethanolamine hydrochloride buffer at pH 6.0 and 30 mM NaCl). ^{1}H NMR spectra were recorded at 40 °C. After the spectrum of the substrate was recorded (0.5 mL of 80 mM), the reaction was initiated by adding the D15G enzyme and sodium azide to final concentrations of 2.5 mg/mL and 1.2 M, respectively, in a final volume of 0.85 mL. ^{1}H NMR spectra were recorded after 0.5, 2, and 24 h and after 7 days. The assignment of the resonance peaks was based on published data (*24*, *31*).

RESULTS AND DISCUSSION

Sequence Analysis, Cloning, and Purification of XynB3. The *xynB3* gene is a part of the hemicellulolytic system of *G. stearothermophilus* T-6 and is located downstream to the xylan and glucuronic acid utilization gene cluster that was previously characterized (*20*). The gene encodes a 536 amino acid protein with a calculated M_r of 61 898. The sequence of the XynB3 protein was scanned with BLAST (*32*) and showed homology to β-xylosidases that belong to GH family 43. Of the 176 genes currently classified as GH43 glycosidases, XynB3 showed the highest protein homologies to the β-xylosidases from (identity percentages are in parentheses): *Oceanobacillus iheyensis* HTE831 (72%), *Bacillus* sp. KK-1 (66%), *B. subtilis* (65%), *Clostridium acetobutylicum*

Table 1: Purification Table of XynB3

purification step	volume (mL)	total protein (mg)	total activity (units)	specific activity (units mg^{-1})	yield (%)	purification (fold)
cell-free extract[a]	50	1085	26.3×10^3	24.2	100	1
heat treatment	45	316	15.4×10^3	48.7	58	2.0
gel filtration	80	174	11×10^3	63.2	42	2.6

[a] Cell-free extract was obtained from 1 L of overnight culture ($OD_{600} = 15$) of recombinant *E. coli* BL21(DE3) pET9d-*xyn*B3.

(64%), *B. pumilus* IPO (64%), and *Selenomonas ruminantium* (60%). According to the phylogenetic analysis made by Qian et al. (*33*), GH43 enzymes can be divided into four subfamilies, and it appears that XynB3 belongs to group I. The *xynB3* gene does not include any recognizable Gram-positive bacterial signal peptide, as determined by the SignalP server (*34*); thus, XynB3 is intracellular. Other GH43 glycosidases from different sources were found to be either intra- or extracellular (*35*−*37*) and could also be found as part of multidomain enzymes, such as the *xynA* gene from the extreme thermophile *Caldicellulosiruptor*, which contains a GH10 xylanase, four CBDs, and a GH43 arabinosidase (*38*, *39*).

The *xynB3* gene from *G. stearothermophilus* T-6 included the alternative starting codon UUG, followed by UCC (Ser). To improve the overexpression in *E. coli*, the starting codon of the cloned protein was replaced to AUG (Met) and the second residue was replaced to GCC (Ala) (*40*). The cloned gene was overexpressed efficiently using the T7 polymerase expression system, and the gene product was purified using two steps, heat treatment and gel-filtration chromatography (Table 1). Typically, over 150 mg of purified XynB3 were obtained from 1 L of overnight culture, with an overall yield of 42%, a purification factor of 2.6, and over 95% purity, as estimated by SDS−PAGE.

Biochemical Characterization. The apparent M_r of XynB3 in solution was estimated by gel-filtration chromatography calibrated using protein markers of known molecular masses. XynB3 was eluted in an elution volume corresponding to a protein with a M_r of about 180×10^3, suggesting that the protein is a trimer in solution. Similarly, the β-xylosidase from *B. pumilus* IPO (which shares 64% protein sequence identity with XynB3) was also suggested to be a trimer based on gel-filtration chromatography (*41*). However, the GH43 arabinanase from *C. japonicus* (Arb43A) is a dimer based on its crystal structure (*7*). The apparent difference in the oligomeric forms could be explained by the fact that the β-xylosidases from *G. stearothermophilus* and *B. pumilus* show sequence identities of only 26% to the dimeric *C. japonicus* Arb43A, and they are significantly larger than Arb43A, containing about 200 additional residues at their C terminus. In the GH43 classification made by Qian et al. (*33*), the *C. japonicus* Arb43A belongs to group IV, whereas the β-xylosidases from *G. stearothermophilus* and *B. pumilus* belong to group I. It is possible therefore, that the two groups differ in their oligomeric state. In this regard, it was recently shown that the α-glucuronidases from GH67 are divided into three subfamilies, where the proteins from one subfamily are monomers and the proteins from the two other subfamilies are dimers, which form two different dimeric structures (*42*). Alternatively, however, it is also possible that the β-xylosidases from *G. stearothermophilus* and *B. pumilus* are in fact dimers (like the *C. japonicus* Arb43A), but their effective molecular radius is longer than that of an ideal sphere, causing them to elute as larger proteins in the gel-filtration analysis.

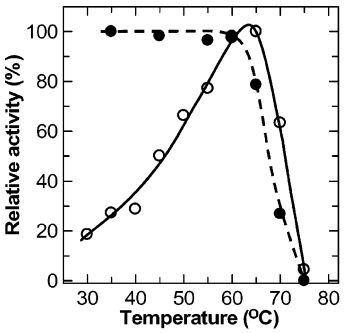

FIGURE 2: Temperature-dependence profile and thermostability of XynB3. The effect of temperature on XynB3 activity was measured at pH 5.0 for 20 min at the given temperatures (○, —). The residual activity after incubating for 30 min at the given temperatures was measured at 40 °C and pH 5.0 (●, - - -).

The optimal temperature for XynB3 activity in a 20 min reaction at pH 5 was 65 °C (Figure 2), and the Arrhenius plot revealed a calculated activation energy of 10 kJ/mol. The enzyme retained full activity up to 60 °C, after incubation of up to 30 min. The activity of XynB3 was not affected by the presence of 1 mM Fe^{3+}, Ca^{2+}, Co^{2+}, Mg^{2+}, Ba^{2+}, Ni^{2+}, K^+, Zn^{2+}, Cu^{2+}, or EDTA, indicating that the enzyme does not require a specific metal ion for its activity. The addition of 1 mM Hg^{2+} has completely inhibited the enzymatic activity, and the addition of 0.1 mM Hg^{2+} and 1 mM Ag^+ has resulted in a residual activity of 7 and 3%, respectively.

Substrate Specificity. Most glycosidases are highly specific with regard to the identity of the substrate glycon, which occupies the −1 subsite at the active site [subsite nomenclature according to Davies et al. (*43*)]. Yet, in family GH43, there are β-xylosidases, α-L-arabinofuranosidases, arabinanases, and xylanases, as well as bifunctional β-xylosidase/α-L-arabinofuranosidase enzymes (*44*−*46*). Other glycosidases from GH families 3, 51, and 54 were also shown to have this polyspecificity between xylo- and arabino-based substrates (*47*, *48*), resulting probably from the spatial similarity of the orientation of the hydroxyl groups and glycosidic bond in β-D-xylopyranosides and α-L-arabinofuranosides. The activity of XynB3 was tested on several synthetic substrates composed of *p*-nitrophenyl (pNP) attached to different sugar units. The highest activity was observed with pNP-β-D-xylopyranoside (pNPX), with k_{cat} of 57 s^{-1}, K_m of 17 mM, and k_{cat}/K_m of 3.3 s^{-1} mM^{-1} at pH 7.0 and 40 °C. The catalytic activity of XynB3 with pNP-α-L-arabinofuranoside as a substrate was 4.5% of the activity with pNPX, with k_{cat} of 2.6 s^{-1}, K_m of 6 mM, and k_{cat}/K_m of 0.43 s^{-1} mM^{-1}, under the same conditions. With other sugar units as the glycons, including β-D-galactopyranoside, α-L-arabinopyranoside, α-L-rhamnopyranoside, β-D-fucopyranoside, β-D-glucopyrano-

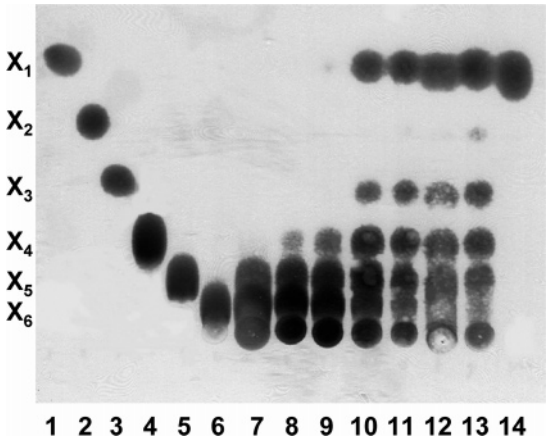

FIGURE 3: Hydrolysis of X_6 by XynB3. TLC analysis of the reaction products. The reaction included 8.3 mM X_6 and 0.3 mg/mL XynB3. Lanes 1−6, X_1, X_2, X_3, X_4, X_5, and X_6 standards. Lanes 7−14, hydrolysis of X_6 by XynB3 after 0.1, 0.5, 1, 3.5, 5, 6.5, 8.5, and 20 h. respectively, at 40 °C and pH 7.0.

side, and β-D-mannopyranoside, XynB3 had less than 0.05% activity compared to pNPX.

Glycosidases can be also characterized by their endo/exo mode of action: endoglycosidases cleave glycosidic bonds whithin the polysaccharide backbone, while exoglycosidases cleave off mono- or disaccharides either from the reducing or the nonreducing end of the polysaccharide chain. In family GH43, there are endoglycosidases (*49*), exoglycosidases (*50*), and also glycosidases with both modes of action (*36*). To determine the XynB3 mode of oligomer hydrolysis, its activity on xylohexaose (X_6) was monitored by TLC (Figure 3). The first hydrolysis product observed after 6 min was xylopentaose (X_5), followed by xylotetraose (X_4) after 1 h, xylotriose (X_3) and X_1 after 3.5 h, and xylobiose (X_2) after 8.5 h. The final hydrolysis product after full hydrolysis was X_1. These results indicate that XynB3 removes single X_1 units from the terminal ends of the xylooligosacchrides and therefore is an exoglycosidase.

To determine whether XynB3 removes the terminal sugar from the reducing or nonreducing ends of the xylooligomers, the activity on $pNPX_2$ was examined by monitoring the pNP formation spectrophotometricaly and by TLC analysis. At all substrate concentrations tested, the initial rates of pNP formation gradually increased with time, until reaching constant rates (Figure 4A). This complex behavior could be explained only if $pNPX_2$ is first hydrolyzed to give X_1 and pNPX, and the latter is then hydrolyzed to X_1 and pNP. Accordingly, the initial rate enhancement results from the elevation in the pNPX concentration. If pNP was released first, then the rate of its formation should have been constant. In addition, TLC analysis of the $pNPX_2$ hydrolysis by XynB3 revealed that the first hydrolysis product was pNPX, followed by X_1, and at no time, X_2 was formed (Figure 4B). Together, these results indicate that XynB3 removes the terminal unit from the nonreducing end of xylooligomers.

Identification of the Catalytic Residues of XynB3. GH43 glycosidases hydrolyze the glycosidic bond by a single-displacement-inverting mechanism, using two conserved acidic residues (*51*) (Figure 1). One carboxylic acid acts as a general-base catalyst, deprotonating a nucleophilic water molecule that attacks the anomeric carbon of the target sugar from the opposite side of the glycosidic bond. The second

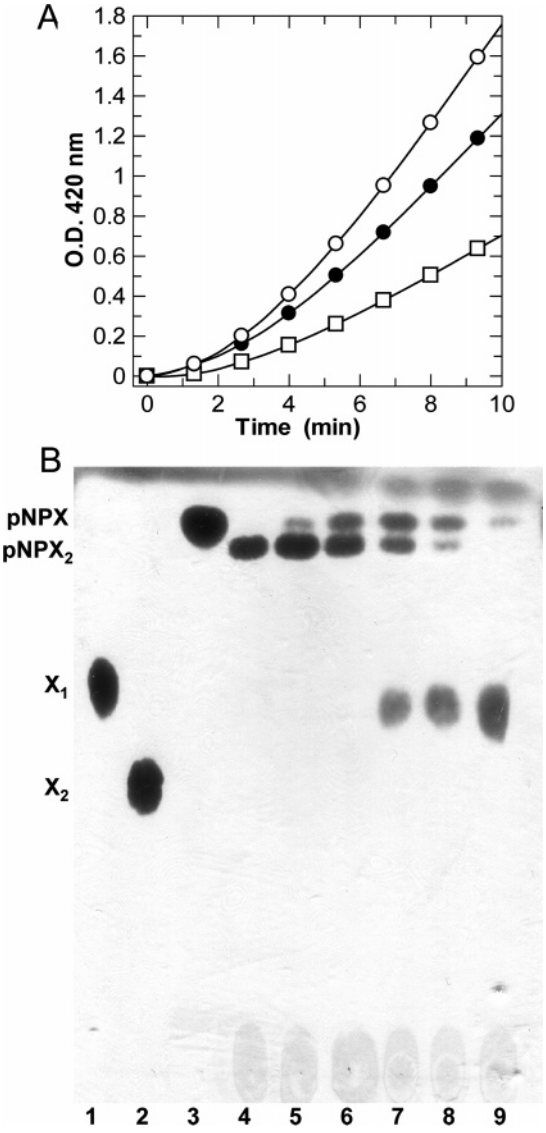

FIGURE 4: Hydrolysis of $pNPX_2$ by XynB3. (A) Spectrophotometric monitoring of pNP formation during the hydrolysis reaction, at different concentrations of $pNPX_2$. ○, 1 mM $pNPX_2$; ●, 0.7 mM $pNPX_2$; and □, 0.36 mM $pNPX_2$. The reactions were performed at 40 °C and pH 7.0. (B) TLC analysis of the reaction products. Lane 1, X_1 standard; lane 2, X_2 standard; lane 3, pNPX standard; lane 4, $pNPX_2$ standard; lanes 5−9, hydrolysis of $pNPX_2$ by XynB3 after 2, 7, 15, 20, and 25 min, respectively, at 40 °C and pH 7.0.

carboxylic residue acts as a general-acid catalyst, protonating the leaving aglycone group (*5*, *6*).

The crystal structure of the *C. japonicus* Arb43A in complex with its substrate arabinotriose revealed three carboxylic acids located near the scissile glycosidic bond. On the basis of the relative positions of these residues and of the substrate, it was proposed that Glu221 is the catalytic acid, Asp38 is the catalytic base, and Asp158 is involved in pK_a modulation and orientation of Glu221 (residues numbered according to the Arb43A sequence) (*7*). Indeed, the replacement of these residues to Ala in Arb43A have resulted in a 6−7 orders of magnitude decrease in the activity compared to the wild-type enzyme, confirming that these residues are essential for catalysis. These three residues are completely conserved and are a part of conserved blocks not only in GH43 proteins but also in GHs 32, 62, and 68 (*10*−*12*). Interestingly, while GH43 and 62 belong to clan GH-F,

Table 2: Kinetic Parameters for Hydrolysis of Aryl-β-D-xylopyranosides by XynB3 and Its E187G Mutant

aglycone	pK_a	enzyme	k_{cat} (s^{-1})	ratio k_{cat} [WT/E187G]	K_m (mM)	k_{cat}/K_m (s^{-1} mM^{-1})	ratio k_{cat}/K_m [WT/E187G]
2,5-dinitrophenyl	5.15	WT	25	0.8	6.3	4.0	1.5
		E187G	30		11	2.7	
3,4-dinitrophenyl	5.36	WT	77	43	3.5	22	6.7
		E187G	1.8		0.55	3.3	
4-nitrophenyl	7.18	WT	57	4071	17	3.3	1222
		E187G	0.014		5.2	2.7×10^{-3}	
4-methylumbelliferyl	7.53	WT	20		2.6	7.7	1100
		E187G	nd[a]		nd	nd	
3-nitrophenyl	8.39	WT	nd		nd	1.8	900×10^3
		E187G	1.0×10^{-5}		5.0	2.0×10^{-6}	
4-bromophenyl	9.34	WT	nd		nd	0.48	
		E187G	$<1.0 \times 10^{-5}$		nd	nd	
2-naphthyl	9.51	WT	nd		nd	0.13	
		E187G	$<1.0 \times 10^{-5}$		nd	nd	
3,4-dimethylphenyl	10.32	WT	nd		nd	0.02	
		E187G	$<1.0 \times 10^{-5}$		nd	nd	

[a] nd = not determined.

families 32 and 68 were assigned to clan GH-J and perform the catalysis using the retaining mechanism. Recently, the crystal structures of enzymes from GHs 32 and 68 revealed that they also share a five-bladed β-propellers fold, similar to that of the GH43 *C. japonicus* Arb43A (*8*, *9*). Structural comparison of the three structures indicated that the three conserved carboxylic acids can be superimposed to give very similar catalytic-site architecture. Remarkably, it appears that what actually determines whether these enzymes operate in an inverting mechanism (GH43) or a retaining mechanism (GHs 32 and 68) is the different ways by which the substrates are positioned in the active site (*8*). More commonly, retaining and inverting glycosidases differ one from another in the distances between the two catalytic residues, about 9 Å in inverting and about 5 Å in retaining enzymes (*52*).

The three conserved residues in XynB3 are Glu187 (putative catalytic acid), Asp15 (putative catalytic base), and Asp128 (pK_a modulation). To date, there is still no biochemical data to support the suggested role of these residues. To identify the exact catalytic function of the residues, they were replaced to Gly, and the resulting mutants were subjected to detailed kinetic analysis.

Activity toward Substrates Bearing Different Leaving Groups. Different arylglycosides, which are synthetic substrates widely used with glycosidases, are distinguished by the pK_a of their aglycon leaving group: the lower the pK_a, the better the leaving group is. Kinetic analysis with such substrates provides one of the major strategies for mechanistic characterization and identification of the catalytic residues of glycosidases. Most commonly, this approach was applied almost exclusively on retaining glycosidases, which operate through a double-displacement mechanism. In this mechanism, the aglycon group is cleaved during the first step of the reaction; therefore, only the rate of this step (glycosylation) is influenced by the leaving-group ability of the substrate. The rate-limiting step of the reaction could be determined by measuring the dependence of k_{cat} on the pK_a of the leaving group. A comparison of these values for wild-type and mutant enzymes has enabled the identification of the acid−base catalytic residues in many retaining glycosidases (*53*, *54*). Inverting glycosidases use a single-displacement S_N2 mechanism, in which the leaving group departs simultaneously with the attack of the nucleophilic water (Figure 1). Therefore, the reactivity of the substrate should affect the rate of the reaction; i.e., k_{cat} should decrease as the pK_a of the leaving group increases. Assuming that the values of the association and dissociation constants of the Michaelis complex (k_1 and k_{-1}) do not depend on the reactivity of the substrate, then k_{cat}/K_m, which equals $(k_2k_1)/(k_2 + k_{-1})$, should also decrease when k_2 decreases. In a catalytic mutant in which the general-acid residue has been removed, there is no activation of the leaving aglycon, and therefore, the reactivity of the substrate will have much greater influence on the activity of the enzyme (*53*). This kind of analysis was performed with the β-xylosidase from *B. pumilus* PRL B12 (presumably a GH43 glycosidase) and with wild-type and mutants forms of the inverting GH6 endoglucanase A from *Cellulomonas fimi* and cellobiohydrolase from *Trichoderma reesei* (*13*, *55*, *56*).

The steady-state values of k_{cat}, K_m, and k_{cat}/K_m for XynB3 and its E187G mutant are presented in Table 2, and the resulting Brønsted plots, correlating log k_{cat} or log k_{cat}/K_m to the pK_a of the leaving group, are shown in Figure 5. For the wild-type XynB3, the k_{cat} values showed no dependency on the leaving-group ability of the substrate and the k_{cat}/K_m values showed only little dependency, with a relatively low Brønsted coefficient (β_{lg}) of −0.46. Similar results were obtained with the β-xylosidase from *B. pumilus* PRL B12, where the calculated Brønsted coefficients are around −0.3 for both k_{cat} and k_{cat}/K_m values (*13*).

For the XynB3 E187G mutant, however, much greater dependency of both the activity and efficiency toward the leaving-group ability of the substrate was observed, with Brønsted coefficients (β_{lg}) of −1.9 and −1.8 for k_{cat} and k_{cat}/K_m, respectively. For substrates with excellent leaving groups (such as 2,5-dinitrophenyl) that require little assistance of the general-acid residue for their departure, the activity and efficiency of the E187G mutant were similar to those of the wild-type enzyme. However, with substrates bearing poorer leaving groups, the activities of the mutant were much lower than the wild-type enzyme and in some cases were too low to be measured. The larger absolute β_{lg} values for the E187G mutant as compared with those of the native XynB3 suggest that in the E187G mutant a higher amount of negative charge is developed on the glycosidic oxygen in the transition state. This difference probably results from the little proton donation that the mutant provides, exactly as

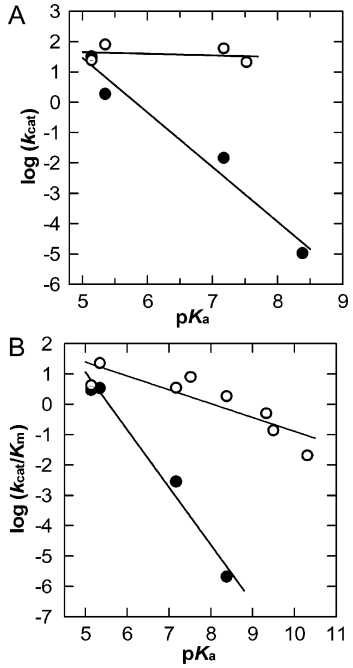

FIGURE 5: Brønsted plots relating turnover numbers and catalytic efficiencies of wild-type XynB3 (○) and its E187G mutant (●), with the leaving-group ability of the substituted phenols. (A) Plot of log(k_{cat}) versus pK_a of the aglycon phenol. (B) Plot of log(k_{cat}/K_m) versus pK_a of the aglycon phenol. The reactions were performed at 40 °C and pH 7.0, in the presence of 10% DMSO.

would be expected in the absence of the acid residue. Overall, these results are in agreement with E187 being the general-acid residue of XynB3.

It is worth noting that the derived absolute β_{lg} values for the general-acid mutant E187G (−1.8 and −1.9) are in fact larger than the value obtained for the spontaneous hydrolysis reaction of 2-aryloxytetrahydropyrans in water ($\beta_{lg} = -1.18$) (*57*). This implies even less proton donation in the mutant than in free solution and could be explained by the hydrophobic character of the +1 subsite environment. Such hydrophobic character of the +1 subsite was also observed in the β-xylosidase from *B. pumilus* PRL B12 (*15*).

For the D15G mutant, the activity on most substrates was too low to determine either k_{cat} or K_m. The hydrolysis of 3,4-dinitrophenyl β-D-xylopyranoside (pK_a = 5.36) and pNPX (pK_a = 7.18) have resulted in similar k_{cat}/K_m values of 1×10^{-5} and 2×10^{-5}, respectively, suggesting that the pK_a of the leaving group has no considerable effect on the activity of D15G, as would be expected from a mutant in the general-base residue.

As described above, Asp128 is the third carboxylic residue that is conserved in all of the glycosidases belonging to clans GH-F and GH-J. The catalytic activity of the XynB3 D128G mutant was lower than that of the E187G and D15G mutants (Table 3), and on most substrates, the activity of D128G was too low to be accurately measured. This result is quite surprising because, in the Arb43A structure, the homologous residue Asp158 is located in such a position that does not allow it to directly participate in catalysis (*7*). However, this residue is only 4 Å from the putative acidic residue Glu221 and about 6.5 Å from the putative basic residue Asp38 and could therefore be involved in pK_a modulation of these two catalytic residues. In addition, Asp158 could potentially make a hydrogen bond with the 3-OH of the sugar in the −1 subsite. Consequently, the removal of this residue could influence the ionization state of both catalytic residues, as well as substrate binding, resulting in major decreases in the activity observed for the Arb43A D158A (*7*) and the XynB3 D128G mutants.

Table 3: Activity of XynB3 and Its Mutants with 3,4-Dinitrophenol Xylopyranoside (pK_a = 5.36) as the Substrate

enzyme	activity at 10 mM substrate [units (mg^{-1} of protein)]	k_{cat}/K_m (s^{-1} mM^{-1})
wild type	37	22
E187G	0.8	3.2
D15G	0.001	1×10^{-5} [a]
D128G	0.0002	4×10^{-5} [a]

[a] These values were estimated at low substrate concentrations.

Interestingly, unlike XynB3, where the E187G mutant had higher activity than the D15G mutant, the activity of the mutant in the putative base of the *C. japonicus* Arb43A (D38A) was higher than the activity of the mutant in its putative acid (E221A). While D38A exhibited 3.5×10^{-6} of the wild-type enzyme activity toward linear arabinan, the activity of the E221A mutant was even lower, $<10^{-7}$ of the wild-type activity (*7*). The difference of this activity pattern compared to the activities of the XynB3 mutants results probably from the different substrates used: Arb43A mutants were tested against the natural substrate arabinan, whereas the activities of the XynB3 mutants were tested against synthetic substrates with substituted phenols as the leaving groups. In the natural substrate, the leaving group is an arabinose unit, which is a very poor leaving group with a pK_a of around 14−16. Because the activity of a mutant in the acidic residue is influenced considerably by the reactivity of the leaving group, it is reasonable that with natural substrates the activity of the acid mutant will be very low. For XynB3, if we extrapolate the Brønsted plots of the wild type and the E187G mutant to substrates with pK_a values of 14 (Figure 5), then indeed the k_{cat} and k_{cat}/K_m values of E187G will be 13 orders of magnitude lower than the wild-type values.

pH-Dependence Activity Profiles. pH-dependence activity profiles of glycosidases are typically bell-shaped, reflecting the ionization state of the two carboxylic catalytic residues in the active site. Elimination of one of the catalytic residues should result in the removal of the corresponding limb from the profile. That is, in a general-acid mutant, the profile should reflect the ionization of only the general-base residue and vice versa (*53*). The kinetic constants of XynB3 and its mutants were determined at different pH values (Figure 6). The pH-dependence profiles of the wild type are typical bell-shaped curve, with optimal activity at pH 6.5 and almost no activity at pH 8.5 and 3.5. The pK_a values of the general-base and general-acid ionizable groups in the free enzyme, derived from the plot of k_{cat}/K_m versus pH, are 5.3 and 7.1, respectively. Likewise, the pK_a values in the enzyme−substrate complex, derived from the plot of k_{cat} versus pH, are 4.5 and 7.2.

The pH-dependence profiles of the E187G mutant were completely different: at pH values of 5.5−9.0, the k_{cat} values changed only slightly and the k_{cat}/K_m values were constant. Unfortunately, determination of the activity of this mutant at pH values lower than 5.5 was not feasible, because the protein precipitated rapidly. Regardless, the absence of the

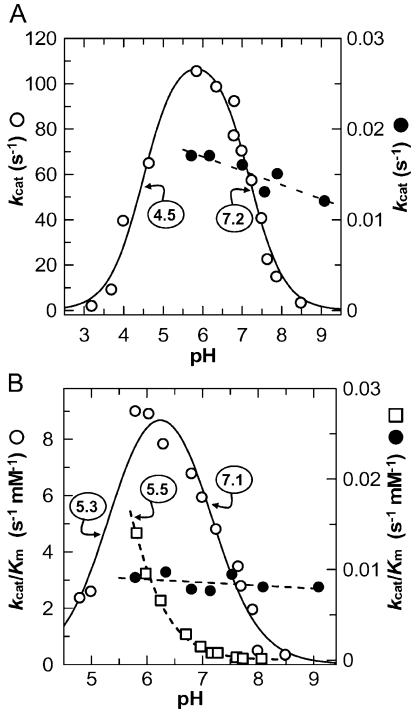

FIGURE 6: pH dependence of the kinetic parameters for the hydrolysis of pNPX by XynB3 (○), XynB3 E187G mutant (●), and XynB3 D15G mutant in the presence of 1 M sodium azide (□). At pH values lower than 5.5, the activity of the mutant proteins could not have been determined because of protein precipitation. The numbers next to the curves are the pK_a values of the ionizable groups, as determined by fitting the data to pK_a equations, using GraFit 5.0. (A) Plot of k_{cat} versus pH. (B) Plot of k_{cat}/K_m versus pH.

basic limb of the curve for this mutant suggests that the protonated catalytic residue had been removed, in agreement with Glu187 being the general-acid residue. Similar behavior was observed also for the general-acid mutant of the inverting GH6 endoglucanase A from *C. fimi* (*58*) and for many acid−base mutants of retaining glycosidases from various families (*21*, *48*, *59*−*61*).

The catalytic activity of the D15G mutant was too low for measuring its pH dependency. However, because the exogenous nucleophile azide has rescued the activity of this mutant (as described below), the addition of 1 M sodium azide to the reaction has made it possible to determine the activity at pH values between 5.5 and 8.0. It was not possible to reach lower pH values at this azide concentration, even with very acidic buffers. The K_m of this mutant in the presence of azide seemed to be very high, and even at 40 mM pNPX, the activity was still in the linear part of the Michaelis−Menten plot (first-order kinetics). Therefore, only k_{cat}/K_m values were estimated. The resulting pH-dependence profile shows that the D15G activity in the presence of sodium azide decreased considerably as the pH was raised. Although the ionization curve was incomplete and included only the basic limb, the pK_a corresponding to an ionization state of a protonated group could be estimated to be around 5.5 and is probably attributed to the general-acid catalyst (Figure 6B). This pH-dependency profile, together with the very low activity of this mutant, is in agreement with Asp15 being the general-base catalytic residue. In addition, it appears that the removal of the general-base Asp15 affects the pK_a of the general-acid residue and shifts it from 7.1 in the wild-type enzyme to around 5.5 in the D15G mutant in the presence of sodium azide. Thus, the high pK_a of the general acid in the wild-type enzyme, which is necessary to its function as a proton donor, is maintained by the presence of the nearby general-base residue. It should be noted however, that because the pH-dependence profile of the D15G mutant was determined in the presence of azide, the real pK_a of the general-acid residue (in the general-base mutant) could be different.

In retaining glycosidases, the distance between the two catalytic residues is around only 5 Å, leading to electrostatic repulsion between these two carboxylic groups. This electrostatic repulsion is essential for the correct ionization state of the catalytic residues during the catalytic cycle (*62*). In inverting glycosidases, the distances between the two catalytic residues can vary between 7 and 11 Å (*63*−*66*). In the *C. japonicus* Arb43A structure, the average distance between the two putative catalytic residues Glu221 and Asp38 is 7.1 Å and the shortest distance between two carboxylic oxygens is 5.9 Å. Assuming similar active-site architecture in XynB3, it seems that electrostatic repulsion between the two catalytic residues could also take place.

Azide Rescue. Activity rescue of catalytic mutants with exogenous nucleophiles, like azide ion, is one of the most definitive tools for the identification of the catalytic residues of retaining glycosidases and was used with many retaining GH families (*53*). In retaining glycosidases, an exogenous nucleophile like azide ion could rescue the activity of enzymes with mutations in either the acid−base residue or in the nucleophilic residue, yielding each time a glycosyl-azide product with different anomeric configuration (*67*). In inverting glycosidases, where the hydrolysis proceeds via a single-displacement mechanism, the addition of exogenous nucleophile could potentially reactivate a mutant in the general-base residue but should not reactivate a mutant in the general-acid residue.

The catalytic activities of XynB3 and its mutants were tested after the addition of different concentrations of sodium azide. For the wild type and the two mutants E187G and D128G, no rate enhancement was observed with pNPX after the addition of 1 M sodium azide. However, the hydrolysis rates of pNPX by the putative basic residue mutant (D15G) were significantly accelerated when increasing concentrations of sodium azide were added (Figure 7A). The presence of 1.4 M sodium azide increased k_{cat} by 35-fold, compared to the activity without azide. No rate enhancement was observed with formate as the exogenous nucleophile.

There are two possible mechanisms by which the azide ion could rescue the activity of general-base mutants of inverting glycosidases (Figure 8). The azide ion could replace the nucleophilic water molecule itself and perform direct attack on the anomeric carbon, forming a glycosyl-azide product. Alternatively, the azide ion could replace the general-base residue by activating the nucleophilic water molecule that will attack the anomeric carbon, forming free sugar with inverted anomeric configuration. The latter mechanism was previously proposed for the general-base mutant of the inverting GH14 β-amylase from *B. cereus* (*68*). To determine in which of these two mechanisms the azide ion accelerated the activity of XynB3 D15G, the pNPX hydrolysis by D15G in the presence of 0.375 M sodium azide was monitored by TLC (Figure 7B). The only reaction

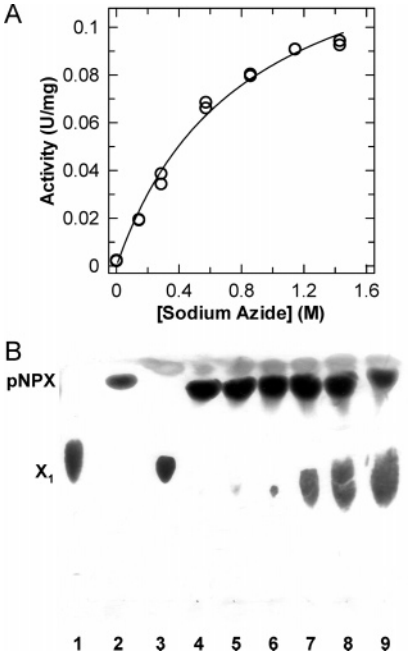

FIGURE 7: Azide rescue of the XynB3 D15G activity. (A) Activity of XynB3 D15G with 45 mM pNPX at different concentrations of sodium azide, at 40 °C and pH 7.0. (B) TLC analysis of the reaction products. Lane 1, X_1 with 0.375 M NaN_3; lane 2, pNPX with 0.375 M NaN_3; lane 3, complete hydrolysis of pNPX to X_1 and pNP by wild-type XynB3; lanes 4−9, hydrolysis of pNPX by D15G mutant in the presence of 0.375 M NaN_3, after 0.3, 1, 2, 3, 4, and 5 h, respectively, at 40 °C and pH 7.0.

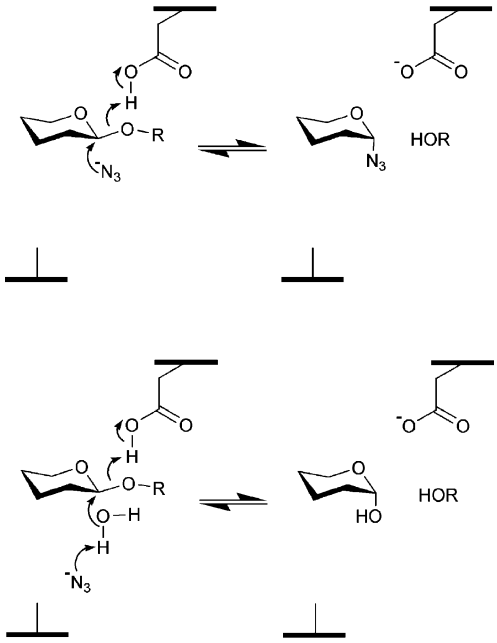

FIGURE 8: Proposed mechanisms for activity rescue of general-base mutants of inverting glycosidases by the exogenous nucleophile azide ion. (Top) Azide ion replaces the nucleophilic water molecule and attacks the anomeric carbon directly, forming the glycosyl-azide product with inverted anomeric configuration. (Bottom) Azide ion replaces the general-base residue by activating the nucleophilic water molecule that subsequently attacks the anomeric carbon, forming free sugar with inverted anomeric configuration.

products observed were pNP and X_1, and no X_1-azide product was detected. To further characterize the hydrolysis products and to try to determine the anomeric configuration of the X_1 moiety formed by the D15G mutant with azide, the reaction was monitored by ^{1}H NMR. Because of the high pNPX concentration used (above 45 mM) and the slow rate of the reaction, the reaction did not reach completion even after 7 days at room temperature. During the reaction, the resonance at 5.10 ppm, which corresponds to the anomeric proton of the substrate, got smaller. Concomitantly, new peaks appeared at 4.45 ppm (J = 8 Hz) and at 5.06 ppm (J = 3.5 Hz), corresponding to the anomeric protons of free α- and β-X_1. At all times measured, the only products observed were the α- and β-X_1 rings and pNP. The ratio between the β and α anomers of the formed X_1 was 1:0.4, which is typical to free X_1 at equilibrium (*24*, *31*). Thus, it seems that enzymatic formation of X_1 by the mutant was slower than the rate of its spontaneous mutarotation, and therefore the initial anomeric configuration of the liberated X_1 could not be determined. Nevertheless, the fact that no X_1-azide intermediate was observed by both TLC and ^{1}H NMR suggests that the azide rescue reaction proceeds through the second mechanism proposed, where the azide ion activates a water molecule to perform the hydrolysis, and not through the formation of a X_1-azide product (Figure 8A).

Interestingly, as suggested from the pH-dependence activity profiles described above (Figure 6), the presence of the negative azide ion did not alter the pK_a of the general-acid residue Glu187 as the general-base residue Asp15 did in the wild-type enzyme. Thus, although the azide ion can replace the general base in the activation of the nucleophilic water molecule, it does not fully imitate the role of Asp15, in agreement with the fact that the azide ion accelerated the D15G mutant only 35-fold, and it did not fully restore the activity to the wild-type level.

In conclusion, the results obtained here indicate that Glu187 and Asp15 are the catalytic acid and base residues of XynB3, respectively. The kinetic activities of the E187G mutant on substrates bearing different leaving groups and the pH-activity dependence profiles of this mutant are characteristic to an inverting glycosidase in which the general-acid residue has been removed. The fact that the addition of the exogenous nucleophile azide ion has rescued the activity of the D15G mutant (but not those of the E187G and D128G mutants) is a clear indication that this residue is the general-base catalytic residue of the enzyme. The result of the D15G pH-activity dependence assay is also in agreement with the suggested role of this residue. Together, the results allow for the first time direct biochemical identification of the catalytic residues of a GH43 glycosidase.

ACKNOWLEDGMENT

We gratefully acknowledge the thoughtful comments of the two anonymous reviewers.

REFERENCES

1. Beg, Q. K., Kapoor, M., Mahajan, L., and Hoondal, G. S. (2001) Microbial xylanases and their industrial applications: A review, *Appl. Microbiol. Biotechnol. 56*, 326−338.
2. Jakeman, D. L., and Withers, S. G. (2002) in *Carbohydrate Bioengineering: Interdisciplinary Approaches* (Teeri, T. T., Svensson, B., Gilbert, H. J., and Feizi, T., Eds.) pp 3−8, The Royal Society of Chemistry, Cambridge, U.K.
3. Shallom, D., and Shoham, Y. (2003) Microbial hemicellulases, *Curr. Opin. Microbiol. 6*, 219−228.

4. Wolfenden, R., Lu, X., and Young, G. (1998) Spontaneous hydrolysis of glycosides, *J. Am. Chem. Soc. 120*, 6814−6815.
5. Davies, G., Sinnott, M. L., and Withers, S. G. (1998) in *Comprehensive Biological Catalysis* (Sinnott, M. L., Ed.) pp 119−209, Academic Press Limited, London, U.K.
6. Sinnott, M. L. (1990) Catalytic mechanisms of enzymic glycosyl transfer, *Chem. Rev. 90*, 1171−1202.
7. Nurizzo, D., Turkenburg, J. P., Charnock, S. J., Roberts, S. M., Dodson, E. J., McKie, V. A., Taylor, E. J., Gilbert, H. J., and Davies, G. J. (2002) *Cellvibrio japonicus* α-L-arabinanase 43A has a novel five-blade β-propeller fold, *Nat. Struct. Biol. 9*, 665−668.
8. Alberto, F., Bignon, C., Sulzenbacher, G., Henrissat, B., and Czjzek, M. (2004) The three-dimensional structure of invertase (β-fructosidase) from *Thermotoga maritima* reveals a bimodular arrangement and an evolutionary relationship between retaining and inverting glycosidases, *J. Biol. Chem. 279*, 18903−18910.
9. Meng, G., and Futterer, K. (2003) Structural framework of fructosyl transfer in *Bacillus subtilis* levansucrase, *Nat. Struct. Biol. 10*, 935−941.
10. Naumoff, D. G. (1999) Conserved sequence motifs in levansucrases and bifunctional β-xylosidases and α-L-arabinases, *FEBS Lett. 448*, 177−179.
11. Naumoff, D. G. (2001) β-Fructosidase superfamily: Homology with some α-L-arabinases and β-D-xylosidases, *Proteins 42*, 66−76.
12. Pons, T., Naumoff, D. G., Martinez-Fleites, C., and Hernandez, L. (2004) Three acidic residues are at the active site of a β-propeller architecture in glycoside hydrolase families 32, 43, 62, and 68, *Proteins 54*, 424−432.
13. Kersters-Hilderson, H., van Doorslaer, E., and de Bruyne, C. K. (1978) β-D-xylosidase from *Bacillus pumilus* PRL B12: Hydrolysis of aryl β-D-xylopyranosides, *Carbohydr. Res. 65*, 219−227.
14. van Doorslaer, E., Kersters-Hilderson, H., and de Bruyne, C. K. (1979) Mechanism of action of β-D-xylosidase from *Bacillus pumilus* PRL B12: pH- and α-deuterium kinetic isotope effects, *Arch. Int. Physiol. Biochim. 87*, 853−854.
15. van Doorslaer, E., Kersters-Hilderson, H., and de Bruyne, C. K. (1980) Binding of alkyl β-D-xylopyranosides, containing branched-chain, cyclic, and substituted aglycon groups, to β-D-xylosidase from *Bacillus pumilus* PRL B12, *Carbohydr. Res. 78*, 317−326.
16. Marshall, P. J., and Sinnott, M. L. (1983) Competitive inhibition of the inverting beta-xylosidase of *Bacillus pumilus* 12 by monosaccharide derivatives of different structural and conformational types. A possible natural substrate, *Biochem. J. 215*, 67−74.
17. Kersters-Hilderson, H., Loontiens, F. G., Claeyssens, M., and de Bruyne, C. K. (1969) Partial purification and properties of an induced β-D-xylosidase of *Bacillus pumilus* 12, *Eur. J. Biochem. 7*, 434−441.
18. Kersters-Hilderson, H., Claeyssens, M., van Doorslaer, E., and de Bruyne, C. K. (1976) Determination of the anomeric configuration of D-xylose with D-xylose isomerases, *Carbohydr. Res. 47*, 269−273.
19. Khasin, A., Alchanati, I., and Shoham, Y. (1993) Purification and characterization of a thermostable xylanase from *Bacillus stearothermophilus* T-6, *Appl. Environ. Microbiol. 59*, 1725−1730.
20. Shulami, S., Gat, O., Sonenshein, A. L., and Shoham, Y. (1999) The glucuronic acid utilization gene cluster from *Bacillus stearothermophilus* T-6, *J. Bacteriol. 181*, 3695−3704.
21. Bravman, T., Belakhov, V., Solomon, D., Shoham, G., Henrissat, B., Baasov, T., and Shoham, Y. (2003) Identification of the catalytic residues in family 52 glycoside hydrolase, a β-xylosidase from *Geobacillus stearothermophilus* T-6, *J. Biol. Chem. 278*, 26742−26749.
22. Bravman, T., Mechaly, A., Shulami, S., Belakhov, V., Baasov, T., Shoham, G., and Shoham, Y. (2001) Glutamic acid 160 is the acid−base catalyst of β-xylosidase from *Bacillus stearothermophilus* T-6: A family 39 glycoside hydrolase, *FEBS Lett. 495*, 115−119.
23. Bravman, T., Zolotnitsky, G., Belakhov, V., Shoham, G., Henrissat, B., Baasov, T., and Shoham, Y. (2003) Detailed kinetic analysis of a family 52 glycoside hydrolase: A β-xylosidase from *Geobacillus stearothermophilus*, *Biochemistry 42*, 10528−10536.
24. Bravman, T., Zolotnitsky, G., Shulami, S., Belakhov, V., Solomon, D., Baasov, T., Shoham, G., and Shoham, Y. (2001) Stereochemistry of family 52 glycosyl hydrolases: A β-xylosidase from *Bacillus stearothermophilus* T-6 is a retaining enzyme, *FEBS Lett. 495*, 39−43.
25. Sambrook, J., Fritsch, E. F., and Maniatis, T. (1989), Cold Spring Harbor Laboratory Press, Cold Spring Harbor, New York.
26. Bradford, M. (1976) A rapid and sensitive method for the quantitation of microgram quantities of protein utilizing the principle of protein-dye binding, *Anal. Biochem. 72*, 248−252.
27. Ziser, L., Setyawati, I., and Withers, S. G. (1995) Syntheses and testing of substrates and mechanism-based inactivators for xylanases, *Carbohydr. Res. 274*, 137−153.
28. Mechaly, A., Belakhov, V., Shoham, Y., and Baasov, T. (1997) An efficient chemical-enzymatic synthesis of 4-nitrophenyl β-xylobioside: A chromogenic substrate for xylanases, *Carbohydr. Res. 304*, 111−115.
29. Leatherbarrow, R. J. (2001) *GraFit 5*, Erithacus Software Ltd., Horley, U.K.
30. Dawson, R. M. C., Elliott, D. C., Elliott, W. H., and Jones, K. M. (1987) *Data for Biochemical Research*, Oxford University Press, Oxford, U.K.
31. Armand, S., Vieille, C., Gey, C., Heyraud, A., Zeikus, J. G., and Henrissat, B. (1996) Stereochemical course and reaction products of the action of β-xylosidase from *Thermoanaerobacterium saccharolyticum* strain B6A-RI, *Eur. J. Biochem. 236*, 706−713.
32. Altschul, S. F., Madden, T. L., Schaffer, A. A., Zhang, J., Zhang, Z., Miller, W., and Lipman, D. J. (1997) Gapped BLAST and PSI-BLAST: A new generation of protein database search programs, *Nucleic Acids Res. 25*, 3389−3402.
33. Qian, Y., Yomano, L. P., Preston, J. F., Aldrich, H. C., and Ingram, L. O. (2003) Cloning, characterization, and functional expression of the *Klebsiella oxytoca* xylodextrin utilization operon (*xynTB*) in *Escherichia coli*, *Appl. Environ. Microbiol. 69*, 5957−5967.
34. Nielsen, H., Engelbrecht, J., Brunak, S., and von Heijne, G. (1997) Identification of prokaryotic and eukaryotic signal peptides and prediction of their cleavage sites, *Protein Eng. 10*, 1−6.
35. Suryani, Kimura, T., Sakka, K., and Ohmiya, K. (2004) Sequencing and expression of the gene encoding the *Clostridium stercorarium* β-xylosidase Xyl43B in *Escherichia coli*, *Biosci. Biotechnol. Biochem. 68*, 609−614.
36. McKie, V. A., Black, G. W., Millward-Sadler, S. J., Hazlewood, G. P., Laurie, J. I., and Gilbert, H. J. (1997) Arabinanase A from *Pseudomonas fluorescens* subsp. *cellulosa* exhibits both an endo and an exo mode of action, *Biochem. J. 323* (part 2), 547−555.
37. Matsuo, N., Kaneko, S., Kuno, A., Kobayashi, H., and Kusakabe, I. (2000) Purification, characterization, and gene cloning of two α-L-arabinofuranosidases from *Streptomyces chartreusis* GS901, *Biochem. J. 346*, 9−15.
38. Gibbs, M. D., Reeves, R. A., Farrington, G. K., Anderson, P., Williams, D. P., and Bergquist, P. L. (2000) Multidomain and multifunctional glycosyl hydrolases from the extreme thermophile *Caldicellulosiruptor* isolate Tok7B.1, *Curr. Microbiol. 40*, 333−340.
39. Morris, D. D., Gibbs, M. D., Ford, M., Thomas, J., and Bergquist, P. L. (1999) Family 10 and 11 xylanase genes from *Caldicellulosiruptor* sp. strain Rt69B.1, *Extremophiles 3*, 103−111.
40. Looman, A. C., Bodlaender, J., Comstock, L. J., Eaton, D., Jhurani, P., de Boer, H. A., and van Knippenberg, P. H. (1987) Influence of the codon following the AUG initiation codon on the expression of a modified lacZ gene in *Escherichia coli*, *EMBO J. 6*, 2489−2492.
41. Xu, W. Z., Shima, Y., Negoro, S., and Urabe, I. (1991) Sequence and properties of β-xylosidase from *Bacillus pumilus* IPO. Contradiction of the previous nucleotide sequence, *Eur. J. Biochem. 202*, 1197−1203.
42. Shallom, D., Golan, G., Shoham, G., and Shoham, Y. (2004) Effect of dimer dissociation on activity and thermostability of the α-glucuronidase from *Geobacillus stearothermophilus*: Dissecting the different oligomeric forms of family 67 glycoside hydrolases, *J. Bacteriol. 186*, 6928−6937.
43. Davies, G. J., Wilson, K. S., and Henrissat, B. (1997) Nomenclature for sugar-binding subsites in glycosyl hydrolases, *Biochem. J. 321*, 557−559.
44. Whitehead, T. R., and Cotta, M. A. (2001) Identification of a broad-specificity xylosidase/arabinosidase important for xylo-oligosaccharide fermentation by the ruminal anaerobe *Selenomonas ruminantium* GA192, *Curr. Microbiol. 43*, 293−298.
45. Utt, E. A., Eddy, C. K., Keshav, K. F., and Ingram, L. O. (1991) Sequencing and expression of the *Butyrivibrio fibrisolvens* xylB gene encoding a novel bifunctional protein with β-D-xylosidase and α-L-arabinofuranosidase activities, *Appl. Environ. Microbiol. 57*, 1227−1234.

46. Sakka, K., Yoshikawa, K., Kojima, Y., Karita, S., Ohmiya, K., and Shimada, K. (1993) Nucleotide sequence of the *Clostridium stercorarium* xylA gene encoding a bifunctional protein with β-D-xylosidase and α-L-arabinofuranosidase activities, and properties of the translated product, *Biosci. Biotechnol. Biochem. 57*, 268−272.
47. Lee, R. C., Hrmova, M., Burton, R. A., Lahnstein, J., and Fincher, G. B. (2003) Bifunctional family 3 glycoside hydrolases from barley with α-L-arabinofuranosidase and β-D-xylosidase activity. Characterization, primary structures, and COOH-terminal processing, *J. Biol. Chem. 278*, 5377−5387.
48. Shallom, D., Belakhov, V., Solomon, D., Gilead-Gropper, S., Baasov, T., Shoham, G., and Shoham, Y. (2002) The identification of the acid−base catalyst of α-arabinofuranosidase from *Geobacillus stearothermophilus* T-6, a family 51 glycoside hydrolase, *FEBS Lett. 514*, 163−167.
49. Skjot, M., Kauppinen, S., Kofod, L. V., Fuglsang, C., Pauly, M., Dalboge, H., and Andersen, L. N. (2001) Functional cloning of an endo-arabinanase from *Aspergillus aculeatus* and its heterologous expression in *A. oryzae* and tobacco, *Mol. Genet. Genomics 265*, 913−921.
50. Gasparic, A., Martin, J., Daniel, A. S., and Flint, H. J. (1995) A xylan hydrolase gene cluster in *Prevotella ruminicola* B_14: Sequence relationships, synergistic interactions, and oxygen sensitivity of a novel enzyme with exoxylanase and β-(1,4)-xylosidase activities, *Appl. Environ. Microbiol. 61*, 2958−2964.
51. Pitson, S. M., Voragen, A. G., and Beldman, G. (1996) Stereochemical course of hydrolysis catalyzed by arabinofuranosyl hydrolases, *FEBS Lett. 398*, 7−11.
52. Zechel, D. L., and Withers, S. G. (2001) Dissection of nucleophilic and acid−base catalysis in glycosidases, *Curr. Opin. Chem. Biol. 5*, 643−649.
53. Ly, H. D., and Withers, S. G. (1999) Mutagenesis of glycosidases, *Annu. Rev. Biochem. 68*, 487−522.
54. Zechel, D. L., and Withers, S. G. (1999) in *Comperhensive Natural Products Chemistry* (Poulter, C. D., Ed.) pp 279−314, Elsevier, New York.
55. Damude, H. G., Withers, S. G., Kilburn, D. G., Miller, R. C., Jr., and Warren, R. A. (1995) Site-directed mutation of the putative catalytic residues of endoglucanase CenA from *Cellulomonas fimi*, *Biochemistry 34*, 2220−2224.
56. Koivula, A., Ruohonen, L., Wohlfahrt, G., Reinikainen, T., Teeri, T. T., Piens, K., Claeyssens, M., Weber, M., Vasella, A., Becker, D., Sinnott, M. L., Zou, J. Y., Kleywegt, G. J., Szardenings, M., Stahlberg, J., and Jones, T. A. (2002) The active site of cellobiohydrolase Cel6A from *Trichoderma reesei*: The roles of aspartic acids D221 and D175, *J. Am. Chem. Soc. 124*, 10015−10024.
57. Craze, G. A., and Kirby, A. J. (1978) The spontaneous hydrolysis of acetals: Sensitivity to the leaving group, *J. Chem. Soc., Perkin Trans. 2 1978*, 354−356.
58. Damude, H. G., Ferro, V., Withers, S. G., and Warren, R. A. (1996) Substrate specificity of endoglucanase A from *Cellulomonas fimi*: Fundamental differences between endoglucanases and exoglucanases from family 6, *Biochem. J. 315*, 467−472.
59. Wang, Q., Trimbur, D., Graham, R., Warren, R. A., and Withers, S. G. (1995) Identification of the acid/base catalyst in *Agrobacterium faecalis* β-glucosidase by kinetic analysis of mutants, *Biochemistry 34*, 14554−14562.
60. MacLeod, A. M., Tull, D., Rupitz, K., Warren, R. A., and Withers, S. G. (1996) Mechanistic consequences of mutation of active site carboxylates in a retaining β-1,4-glycanase from *Cellulomonas fimi*, *Biochemistry 35*, 13165−13172.
61. Li, Y. K., Chir, J., Tanaka, S., and Chen, F. Y. (2002) Identification of the general acid/base catalyst of a family 3 β-glucosidase from *Flavobacterium meningosepticum*, *Biochemistry 41*, 2751−2759.
62. McIntosh, L. P., Hand, G., Johnson, P. E., Joshi, M. D., Korner, M., Plesniak, L. A., Ziser, L., Wakarchuk, W. W., and Withers, S. G. (1996) The pK_a of the general acid/base carboxyl group of a glycosidase cycles during catalysis: A ^{13}C NMR study of *Bacillus circulans* xylanase, *Biochemistry 35*, 9958−9966.
63. van Santen, Y., Benen, J. A., Schroter, K. H., Kalk, K. H., Armand, S., Visser, J., and Dijkstra, B. W. (1999) 1.68-Å crystal structure of endopolygalacturonase II from *Aspergillus niger* and identification of active site residues by site-directed mutagenesis, *J. Biol. Chem. 274*, 30474−30480.
64. Alzari, P. M., Souchon, H., and Dominguez, R. (1996) The crystal structure of endoglucanase CelA, a family 8 glycosyl hydrolase from *Clostridium thermocellum*, *Structure 4*, 265−275.
65. Pickersgill, R., Smith, D., Worboys, K., and Jenkins, J. (1998) Crystal structure of polygalacturonase from *Erwinia carotovora* ssp. carotovora, *J. Biol. Chem. 273*, 24660−24664.
66. Golan, G., Shallom, D., Teplitsky, A., Zaide, G., Shulami, S., Baasov, T., Stojanoff, V., Thompson, A., Shoham, Y., and Shoham, G. (2004) Crystal structures of *Geobacillus stearothermophilus* α-glucuronidase complexed with its substrate and products: Mechanistic implications, *J. Biol. Chem. 279*, 3014−3024.
67. Viladot, J. L., de Ramon, E., Durany, O., and Planas, A. (1998) Probing the mechanism of *Bacillus* 1,3-1,4-β-D-glucan 4-glucanohydrolases by chemical rescue of inactive mutants at catalytically essential residues, *Biochemistry 37*, 11332−11342.
68. Miyake, H., Otsuka, C., Nishimura, S., and Nitta, Y. (2002) Catalytic mechanism of β-amylase from *Bacillus cereus* var. *mycoides*: Chemical rescue of hydrolytic activity for a catalytic site mutant (Glu367 → Ala) by azide, *J. Biochem. 131*, 587−591.

BI048059W